Supplement of Earth Surf. Dynam., 12, 1243–1266, 2024
https://doi.org/10.5194/esurf-12-1243-2024-supplement

Supplement of

River suspended-sand flux computation with uncertainty estimation using water samples and high-resolution ADCP measurements

Jessica Marggraf et al.

Correspondence to: Jessica Marggraf (jmarggra@umn.edu) and Guillaume Dramais (guillaume.dramais@inrae.fr)

S1 Detailed description of the Multitransect Averaged Profile (MAP)

The Acoustic Doppler Current Profilers (ADCP) gauging method is extensively used to measure the discharge and generate a three-dimensional flow map. ADCP discharge measurements are usually the average of individual discharge measurements from successive ADCP transects. Beyond this value of discharge, this process can be extended on the entire transect. ADCP are multipurpose instruments for examining flow, morphology and sediment flux. The increasing use of ADCPs to explore the characteristics of complex natural flows has led to a need for post-processing methods for managing, evaluating, analyzing, and displaying three-dimensional velocity data. The Velocity Mapping Toolbox (VMT) (Parsons et al., 2013) is a tool that permits averaging and visualizing velocity datasets. The VMT method has been developed on Matlab and does not include extrapolated discharge (top/bottom/edges discharge). Coupled to QRevInt (Mueller, 2020; Lennermark and Hauet, 2022), the Multitransect Averaged Profile (MAP) aims to include each transect completely to generate an averaged transect profile from the bottom to the topmost cell. MAP is a method in which multiple transects can be projected and averaged onto a 2D planar grid to allow analysis of the 3D flow field. This methodology is developed with Python and based on QRevInt measurement output.

S1.1 Determine average cross-section and project data

The first step is to define an average cross-section line. MAP can use GGA coordinates to localize ADCP for each ensemble. The GGA sentence is defined by the NMEA 0183 standard (National Marine Electronics Association, 2002). QRevInt computes x and y rectilinear components by computing the Universal Transverse Mercator (UTM) coordinates for the geographic positions. If the ADCP is used with a global positioning system, as is normally recommended for velocity mapping applications particularly with moving-bed conditions (Mueller et al., 2013), each vertical profile of three- dimensional ADCP velocity data is automatically georeferenced during data collection. MAP also works with bottom track and VTG coordinates. However, the starting point of each transect is not georeferenced. It computes distance on x and y rectilinear components from the starting point. To have the same origin point regardless of the starting edge, the left-most point of each transect is used as the origin point. This approximation is temporary, a correction will be applied later (Section S1.2). Every navigation reference uses the same method to compute an average cross-section. It is defined by the first and the last point of each transect. The two median points (one on the left edge, the other one on the right edge) allow to define a straight line which is the average ship track used by MAP (Figure S1).

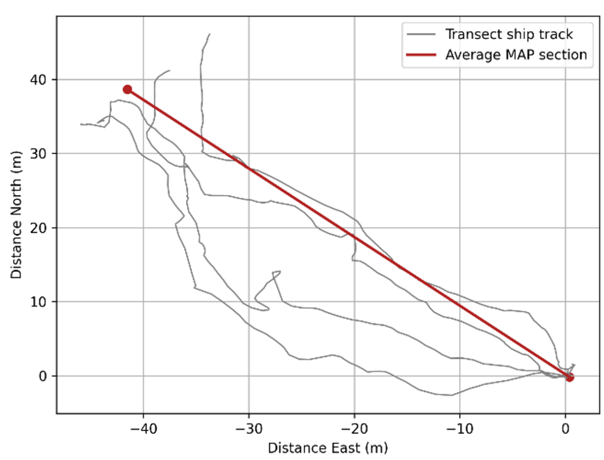

Figure S1: Average cross-section defined by extreme points.

Two other approaches have been tested but the orientation of the line could be inconsistent in many cases (see Appendix A). Then, MAP projects data on the average cross-section following equations S1 and S2.

$$X_{\text{proj}} = \frac{X - ab + aY}{a^2 + 1} \tag{S1}$$

$$Y_{\text{proj}} = \frac{b + aX + a^2Y}{a^2 + 1} \tag{S2}$$

with X and Y respectively East and North coordinates, X_{proj} and Y_{proj} respectively East and North coordinates on the average cross-section defined by $Y = aX + b$. At this stage, the reference is now the average cross-section plan.

S1.2 Bathymetry matching and define a mesh grid

For BT and VTG reference, to compare similar data, MAP has to check if the bathymetry of selected transects is consistent. The first step to compare bathymetry is to use a same size data set. MAP divides the average cross-section in 100 segments between the two extreme points. For each transect, a linear interpolation permits to assign a depth value to each segment as illustrated in Figure S2.

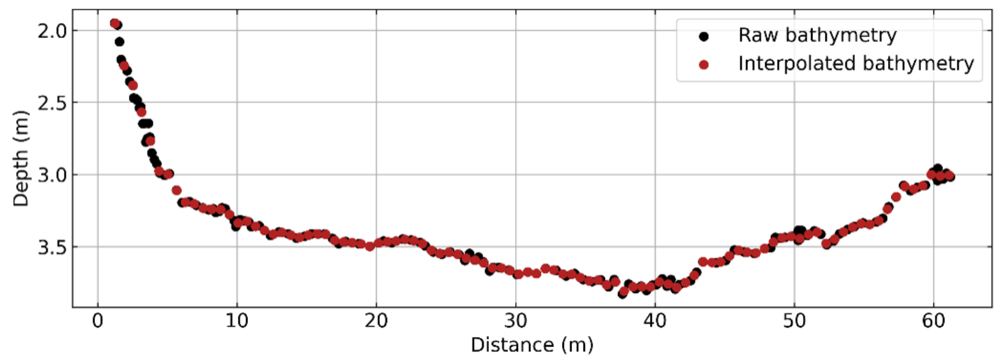

Figure S2: Raw bathymetry (ensembles) and interpolated bathymetry for the 100-segments-subdivision.

The longest transect is used as reference. Other interpolated transects are compared to it. To minimize the mean square difference between them, a translation is done to find the best position. For instance, in Figure S3, the interpolated bathymetry of the transect n (light blue dots) has a shift of 4 meters with the reference interpolated bathymetry (red dots). Then, MAP applies a translation on the data of the transect n (dark blue dots).

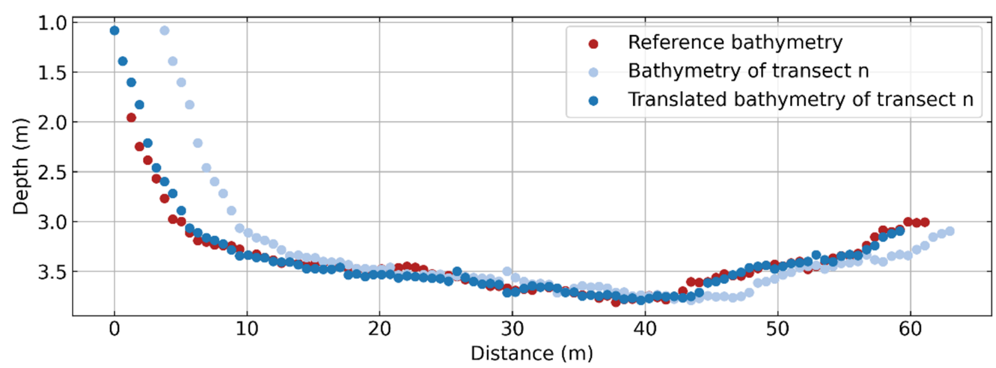

Figure S3: Correction for the transect n according to its bathymetry compared to the reference bathymetry.

Once each transect is properly positioned, MAP defines a homogeneous 2D planar grid. If the user specified mesh size on length and/or depth, it applies user's value. Otherwise, mesh's length is defined as the maximum distance between two cells. Mesh's depth is computed as twice the different in depth of the ADCP's cells.

S1.3 Compute mean profile

At this point, a homogeneous grid has been computed on each transect. To assign velocities value to each MAP's mesh, it computes median value from cells which have their center in the mesh. In Figure S4, the MAP's mesh (red rectangle) takes the value of the median of the 9 cells which have their center inside (blue dots). For depths, a similar process on ensembles is applied.

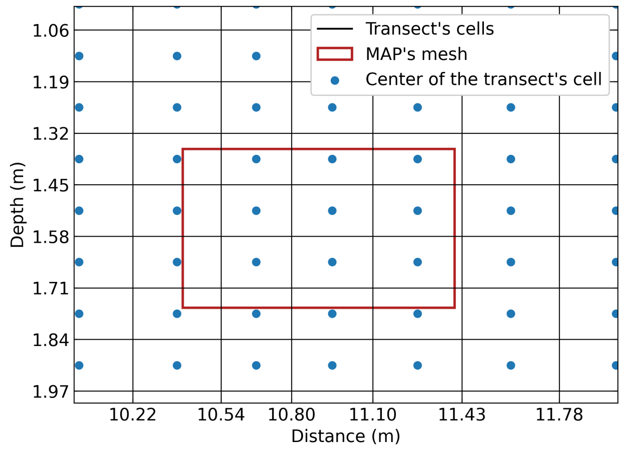

Figure S4: Schematic representation of a MAP's mesh and transect's cells.

Once all transects are averaged on the homogeneous grid, MAP overlaps them to compute mean on each mesh for basic variables (North, East and vertical velocity components and depth) as shown in Figure S5. To avoid overestimating, only verticals detected by at least a third of transects are computed (if three or more transects are used). Logically, velocities are computed only if the mesh is above the streambed.

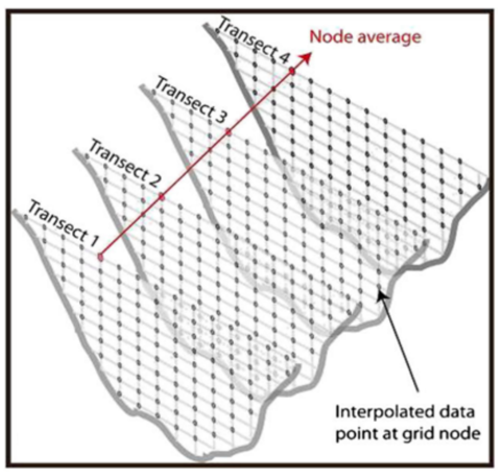

Figure S5: Compute median of all transects at each grid mesh for velocities components (Parsons et al., 2013).

Then, North and East velocity components are transformed into primary and secondary velocities according Rozovskii's projection (Rozovskii, 1957). It is one way to isolate skewed flow from helical motion. Primary and secondary velocities are respectively velocity components parallel and perpendicular to the averaged velocity vector ($\overline{V_{\text{ens}}}$) at each vertical.

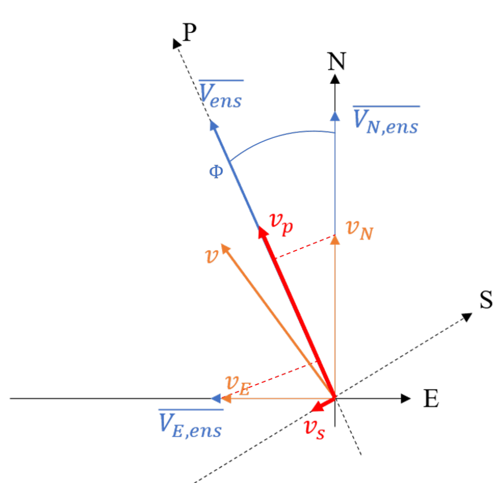

Figure S6: Diagram illustrating relations among averaged East velocity ($\overline{V_{\text{E,ens}}}$), averaged North velocity ($\overline{V_{\text{N,ens}}}$), resultant velocity ($\overline{V_{\text{ens}}}$) at a vertical, East velocity (v_E), North velocity (v_N), mean resultant velocity (v), the primary velocity (v_p) and the secondary velocity (v_s) at a point in a vertical. Coordinate systems E, N and P, S correspond to the East/North coordinates and primary/secondary flow directions, respectively.

v_E and v_N are respectively East and North velocity components on a mesh. $\overline{V_{\text{E,ens}}}$ and $\overline{V_{\text{N,ens}}}$ are respectively the mean East and North velocity components on the vertical of the mesh. The orientation (Φ) of $\overline{V_{\text{ens}}}$ is calculated as:

$$\Phi = \arctan\left(\frac{\overline{V_{\text{N,ens}}}}{\overline{V_{\text{E,ens}}}}\right) \tag{S3}$$

Then, primary (v_p) and secondary (v_s) velocity components of each mesh are computed as:

$$v_p = v_E \cos(\Phi) + v_N \sin(\Phi) \tag{S4}$$

$$v_s = v_E \sin(\Phi) - v_N \cos(\Phi) \tag{S5}$$

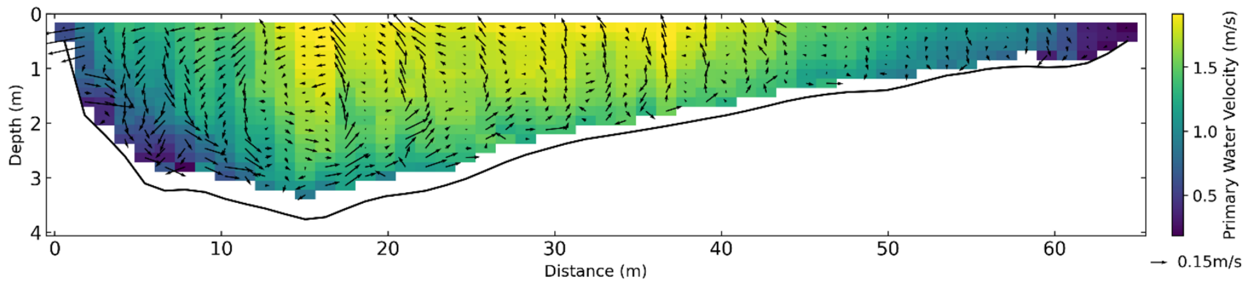

Figure S7: MAP velocity profile for a measurement without edge/top/bottom extrapolation (arrows represent secondary velocities).

S1.4 Extrapolation

To complete the averaged profile, the user can chose if he wants to apply extrapolation. If the extrapolated option is selected, MAP empties meshes that are under 10% of each vertical depth similarly as the side-lob effect (which is between 6 and 13%). For top/bot primary velocity extrapolation, MAP uses QRevInt default extrapolation methods and exponent. As there is no mathematical law for secondary and vertical velocities, they are respectively extrapolated following constant law and linear regression to zero at free surface/streambed. For edges extrapolation, banks are divided into same shape meshes as the middle streamflow. Mean primary velocity ($\overline{V_x}$) on each edge's vertical is computed according to power law:

$$\overline{V_x} = \overline{V_{0/\text{n}}}\left(\frac{x}{L_{\text{edge}}}\right)^{\frac{1}{m_{\text{edge}}}} \tag{S6}$$

Where x is the distance of the vertical from the start of the bank, L_{edge} is the length of the edge, m_{edge} is an edge-shape exponent (2.41 for a triangular edge, 10 for a rectangular edge, edge extrapolation is not computed otherwise) and $\overline{V_{0/\text{m}}}$ the mean primary velocity from the closest measured vertical. Then, primary velocity on each edges' mesh (v_p) is computed following power law with QRevInt extrapolation exponent (m_{extrap}):

$$v_p = \overline{V_x}\frac{m_{\text{extrap}} + 1}{m_{\text{extrap}}}\left(\frac{z}{d}\right)^{\frac{1}{m_{\text{extrap}}}} \tag{S7}$$

Where z is the depth to centerline of mesh and d the depth on the vertical of the edge. Secondary velocity edges extrapolation uses a linear law from the closest middle vertical to zero at edge. Vertical velocity on edge follows the distribution of vertical velocities on the closest middle vertical.

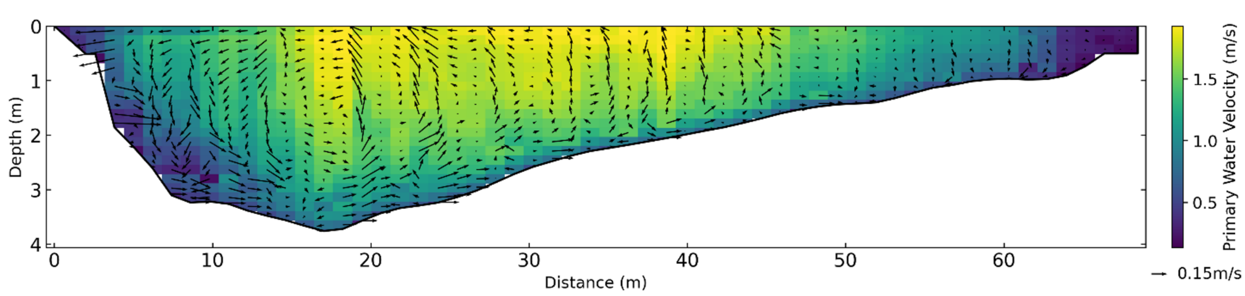

Figure S8: MAP velocity profile with extrapolation (arrows represent secondary velocities).

S1.5 Discharge

The discharge is computed perpendicularly to the average cross-section. MAP projects primary and secondary velocities normally to this section (Figure S9) defined by the equation $Y = aX + b$ as explained in Section S1.1. The orientation (δ) of discharging velocity is defined by:

$$\delta = \frac{-1}{a} \tag{S8}$$

Then, MAP computes streamwise velocity:

$$v_q = v_p \cos(\Phi - \delta) + v_s \sin(\Phi - \delta) \tag{S9}$$

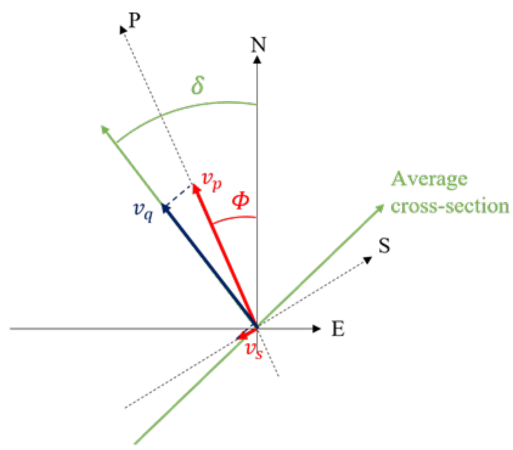

Figure S9: Diagram illustrating relations among the primary velocity (v_p), the secondary velocity (v_s) and the streamwise velocity (v_q) at a point in a vertical. Coordinate systems E, N and P, S correspond to the East/North coordinates and primary/secondary flow directions, respectively.

Finally, discharge through each mesh is computed as $Q_{\text{mesh}} = A_{\text{mesh}} v_{\text{q,mesh}}$ with A_{mesh} the area of each mesh. Bottom meshes on the middle part are rectangles whose width stops when it reaches streambed. Edge meshes are rectangular a rectangular shape is selected. Otherwise, if a triangular edge shape is selected, meshes can have various shapes depending on how edge streambed cuts the mesh.

S1.6 Results

Mean profiles from MAP and ADCP transects have been compared according to their discharge. In Figure S10, measurements from five intercomparisons experiments has been used. It compares the relative discharge difference between MAP averaged profile and QRevInt mean value for each measurement. These results have been computed with MAP default methodology and with checked transects from the raw measurement. The operator could improve them with coherent selection. Absolute median deviation, on these 164 measurements is -0.4% (90% interval is [-5.4%, 3.8%]). However, some measurements have wrong transects or MAP default depth layer is not adapted. In this study example, differences lower than -6.5% are caused by inconsistent depth layer or loop in a single transect. On the other hand, differences higher than 6.9% are caused by transect's discharge at zero or just bad measurement.

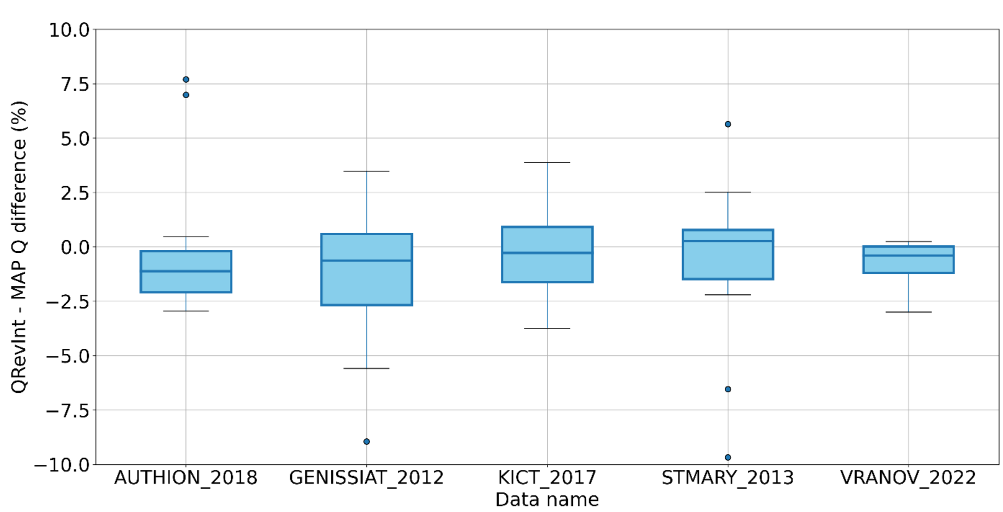

Figure S10: Discharge relative difference for 5 intercomparisons between QRevInt and MAP in default mode.

However, MAP cannot properly compute average profile for measurements without compass. It results in irrelevant boat trajectories as illustrated in Figure S11. It will not be available in QRevInt if the conditions are not fulfilled.

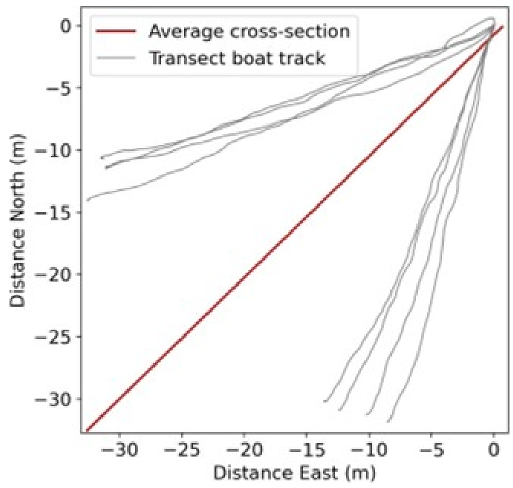

Figure S11: Incoherent Stream Pro average cross-section defined by boat coordinates and linear regression.

S1.7 QRevInt

QRevInt has a new tab for MAP profile. On the top-left part, user can change parameter of MAP: cells properties, top/bottom/edge extrapolation, use interpolated data. It is also possible to change the figure to show bed profile by transect, to plot primary or streamwise velocity and add quivers for secondary/transverse velocity. Once changes are made, the user simply needs to click on "Apply" button to update the tab.

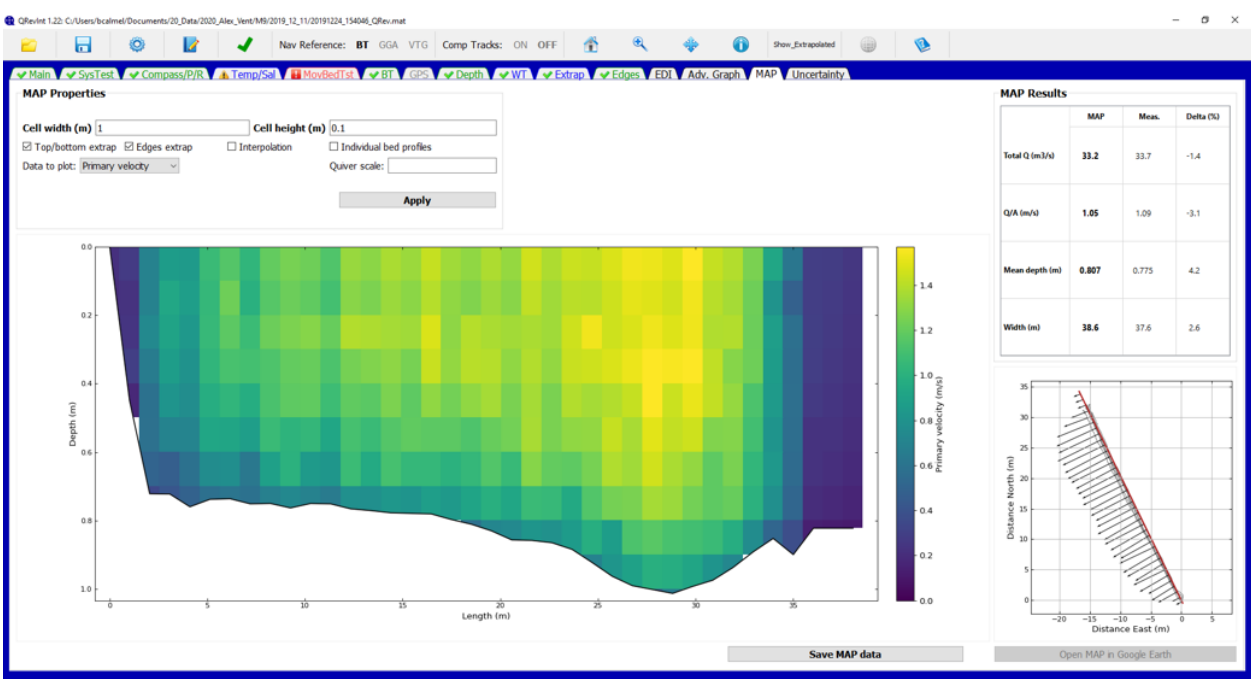

Figure S12: MAP tab in QRevInt (Mueller, 2020b).

MAP's implementation was also the opportunity to save figures from QRevInt as png, jpeg, pdf or svg. Now, every graph in QRevInt can be locally saved with a right click on it. It is possible to export MAP data as csv (separator semicolon) or txt (space separator) with the "Save MAP data" button under profile figure. On the top-right part, there is a table with the main MAP results and the comparison with QRevInt measurement. Total discharge and width are particularly interested to warn if there is an inconsistence between MAP and QRevInt. However, Q/A and mean depth are not very relevant because MAP's cells are uniformed while it is not the case for raw cells. Finally, on the bottom-right part, there is a figure of ship track (transects in grey), and the MAP average ship track straight line in red. If the measurement is in GGA navigation reference, the button under this graph is enabled to see MAP section in Google Earth (Figure S13).

Figure S13: MAP average ship track and transects opened in Google Earth (picture from © Google Earth).

S1.8 Tested approaches to determine the average ship course

S1.8.1 Weighted linear regression on boat coordinates

Each vertical has a weight defined as the discharge of the ensemble normalized by the mean discharge of the transect (Figure S14). Linear regression is applied to each transect to establish linear equation $y = ax + b$. Then, median a and b are used to compute average cross-section's equation. The limitation of this method is the influence of areas with high concentration of points which can lead to error.

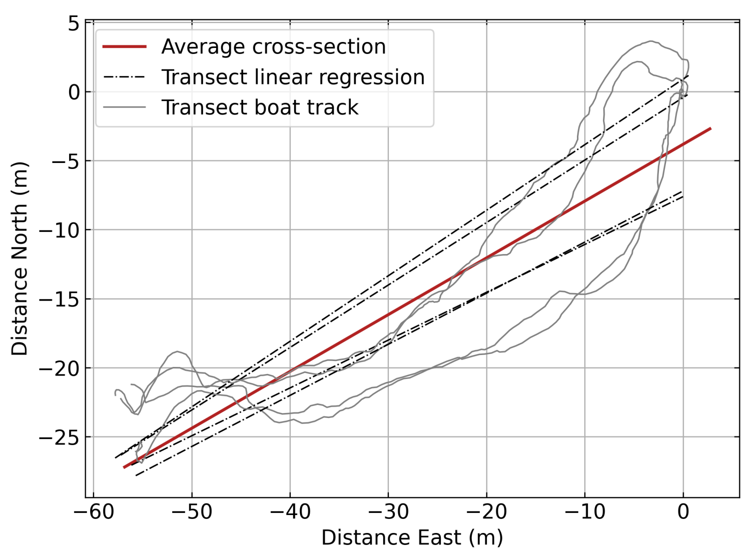

Figure S14: Average cross-section defined by boat coordinates and linear regression.

S1.8.2 Determine the mean cross-stream velocity-orientation

In the other case, on each transect MAP compute the weighted average velocities (North and East) by discharge (Figure S15). For a transect m with j ensembles and i depth layers:

$$v_m = \frac{\sum_{i,j} v_{i,j} q_{i,j}}{\sum_{i,j} q_{i,j}} \tag{S10}$$

MAP computes median of the weighted average transect velocities in order to define the main downstream flow direction δ:

$$\delta = \arctan\left(\frac{v_{\mathrm{m,N}}}{v_{\mathrm{m,E}}}\right) \tag{S11}$$

With $v_{\mathrm{m,N}}$ and $v_{\mathrm{m,E}}$ median values respectively on North and East direction. The slope coefficient a is defined as:

$$a = \frac{-1}{\tan\delta} \tag{S12}$$

Finally, a least squares regression permits to determine the best intercept b according to boat tracks and the slope coefficient. This approach is consistent only with straight streams, but it is frequently not representative of transects.

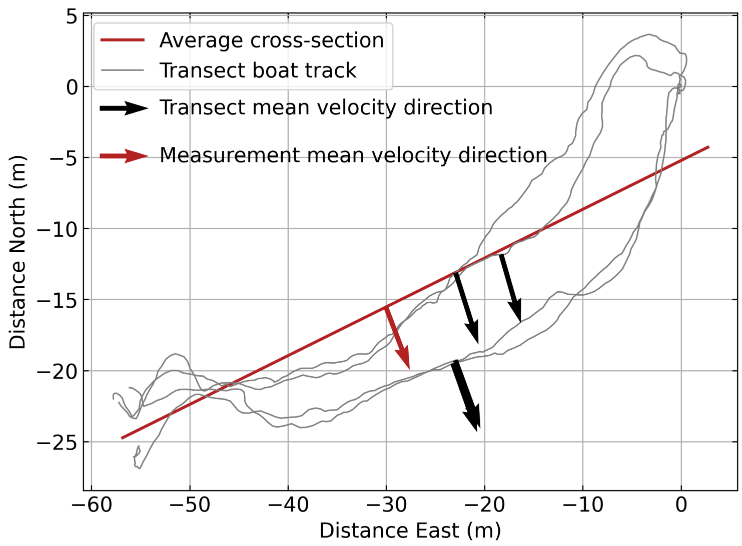

Figure S15: Average cross-section defined by mean velocity direction.

S2 Comparing the empirically-fitted Rouse profile

The presented toolbox includes also a method similar to the SDC method using the Rouse profile (Rouse, 1937). Instead of using the exponential profile of (Camenen et al, 2008) and the Bayesian modeling BaM! (Mansanarez et al., 2019), in this so-called SDC-Rouse method, the Rouse profile is fitted empirically to the data points. Except this more traditional and widely used approach for the vertical integration, the lateral integration and determination of the point concentration remain the same.

The relative differences $\epsilon_{\Phi,\mathrm{Rouse-ISO}}$ and $\epsilon_{\Phi,\mathrm{SDC-Rouse}}$ between the sand fluxes estimated using the SDC-Rouse method Φ_{Rouse} and the ISO Φ_{ISO} or SDC Φ_{SDC} method, respectively, are determined as:

$$\epsilon_{\Phi,\mathrm{Rouse-ISO}} = (\Phi_{\mathrm{Rouse}} - \Phi_{\mathrm{ISO}})/\Phi_{\mathrm{ISO}} \tag{S13}$$

and

$$\epsilon_{\Phi,\mathrm{SDC-Rouse}} = (\Phi_{\mathrm{SDC}} - \Phi_{\mathrm{Rouse}})/\Phi_{\mathrm{Rouse}} \tag{S14}$$

The relative differences $\epsilon_{\Phi,\mathrm{Rouse-ISO}}$ range from -40 to 36 % and show a slight underestimation of the sand fluxes determined using the Rouse profile compared to the ISO method for the Isère River measurements (Figure S16). In contrast, no such bias is visible for the relative differences between the SDC and SDC-Rouse methods, which range from -30 to 32 % (Figure S17). In general, the relative differences between the three different methods (ISO, SDC, SDC-Rouse) are usually smaller than the estimated uncertainty in the flux U'_{Φ}. Except the relative difference $\epsilon_{\Phi,\mathrm{Rouse-ISO}}$ calculated for the Amazon which accounts for 32 % is larger than the uncertainty U'_{Φ} (26.6 %). This shows that the uncertainty in the flux measurement is larger than the difference between the applied methods.

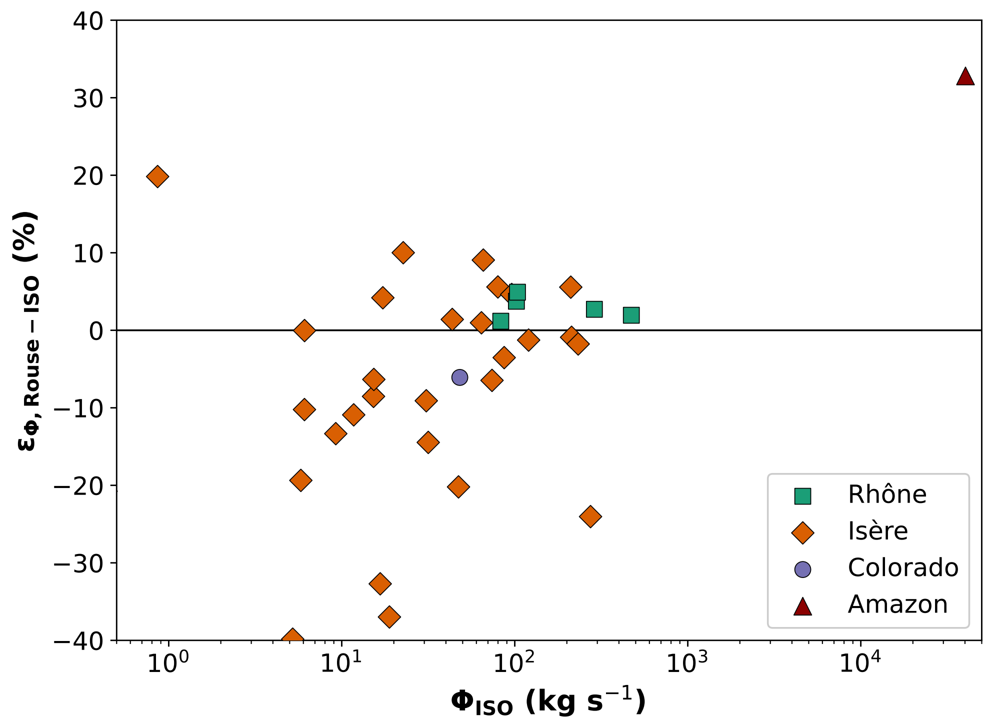

Figure S16: Relative difference $\epsilon_{\Phi,\mathrm{Rouse-ISO}}$ as a function of the suspended-sand flux Φ_{ISO} determined using the ISO method for all four studied rivers, Φ_{Rouse} is determined using an empirically fitted Rouse profile for all four studied rivers.

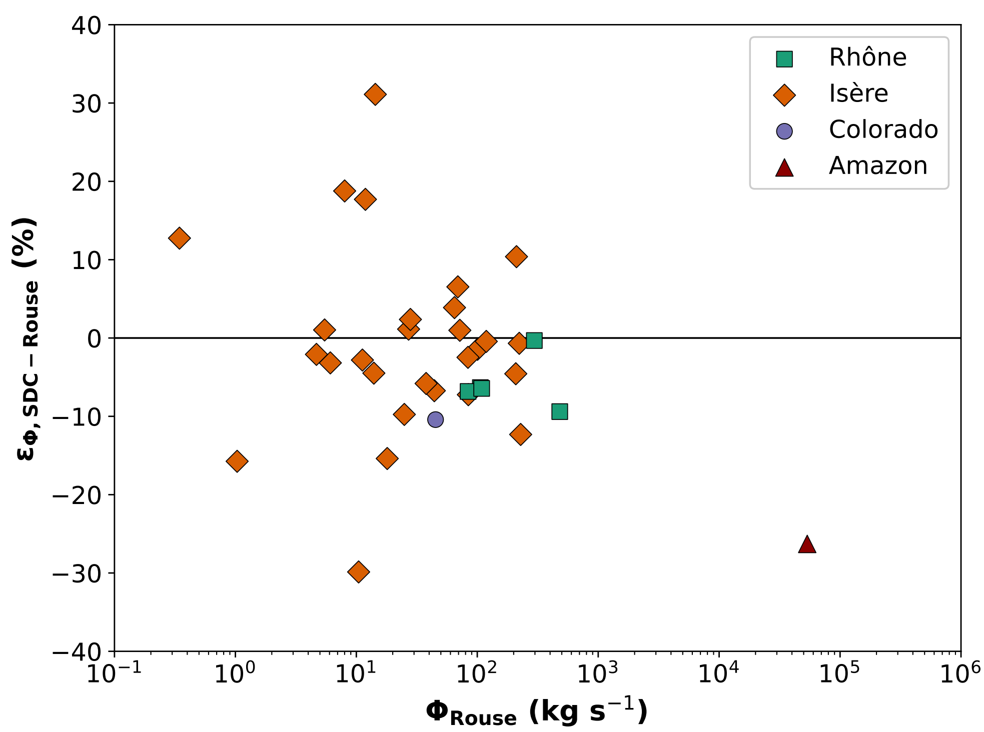

Figure S17: Relative difference $\epsilon_{\Phi,\mathrm{SDC-Rouse}}$ as a function of the suspended-sand flux Φ_{SDC} determined using the SDC method for all four studied rivers, Φ_{Rouse} is determined using an empirically fitted Rouse profile for all four studied rivers.

References

Camenen, B. and Larson, M.: A general formula for noncohesive suspended sediment transport, J. Coastal Res., 24, 615–627, 2008.

Lennermark, M. and Hauet, A.: Developing a post-processing software for ADCP discharge measurement piloted by an international and inter-agency group: a unique, ambitious experience. . . and one that works!, EGU General Assembly 2022, Vienna, Austria, 23–27 May 2022, EGU22-9379, https://doi.org/10.5194/egusphere-egu22-9379, 2022.

Mansanarez, V., Renard, B., Le Coz, J., Lang, M., and Darienzo, M.: Shift Happens! Adjusting Stage-Discharge Rating Curves to Morphological Changes at Known Times, Water Resour. Res., 55, 2876–2899, https://doi.org/10.1029/-2018WR023389, 2019.

Mueller, D.: QRev – Technical Manual. United States Geological Service, https://hydroacoustics.usgs.gov/software/–QRev_Tech_20200924.pdf, last access: 10 April 2024, 2020.

Mueller, D. S., Wagner, C. R., Rehmel, M. S., Oberg, K. A., and Rainville, F.: Measuring discharge with acoustic Doppler current profilers from a moving boat. Techniques and methods 3-a22, United States Geological Service,

https://doi.org/10.3133/tm3A22, 2013.
Parsons, D. R., Jackson, P., Czuba, J., Engel, F., Rhoads, B. L., Oberg, K., Best, J. L., Mueller, D., Johnson, K., and Riley, J.: Velocity Mapping Toolbox (VMT): a processing and visualization suite for moving-vessel ADCP measurements, Earth Surf. Processes, 38, 1244–1260, https://doi.org/10.1002/esp.3367, 2013.
Rouse, H.: Modern conceptions of the mechanics of fluid turbulence, Trans. ASCE, 102, 463–505, 1937.
Rozovskii, I. L.: Flow of waterin bends of open channels, Academy of Sciences of the Ukrainian SSR: Kiev, translated from Russian by the Israel Program for Scientific Translations, Jerusalem, 1961, 1957.